

## Rapid #: -21966205

CROSS REF ID: 26300161490001853

LENDER: **CSA (California State University, Sacramento) :: Main Library**

BORROWER: **ORZ (Portland State University) :: Main Library**

TYPE: Article CC:CCG

JOURNAL TITLE: Thin solid films

USER JOURNAL TITLE: Thin solid films.

ARTICLE TITLE: Optical transmission and photoconductivity of chemical bath-deposited CdS thin films for optoelectronic applications

ARTICLE AUTHOR: Dissanayake, MAKL ; Paramanathan, K ; Senadeera, G

VOLUME: 791

ISSUE:

MONTH:

YEAR: 2024

PAGES: 140225

ISSN: 0040-6090

OCLC #: 1605925

Processed by RapidX: 1/30/2024 5:35:55 PM

---

This material may be protected by copyright law (Title 17 U.S. Code)

---



# Optical transmission and photoconductivity of chemical bath-deposited CdS thin films for optoelectronic applications

M.A.K.L. Dissanayake<sup>a,\*</sup>, K. Paramanathan<sup>a,b</sup>, G.K.R. Senadeera<sup>a,c</sup>, C.A. Thotawattage<sup>a</sup>,  
K. Balashangar<sup>d</sup>, P. Ravirajan<sup>e</sup>, B.S. Dassanayake<sup>f</sup>

<sup>a</sup> National Institute of Fundamental Studies, Kandy, Sri Lanka

<sup>b</sup> Postgraduate Institute of Science, University of Peradeniya, Peradeniya, Sri Lanka

<sup>c</sup> Department of Physics, The Open University of Sri Lanka, Nawala Nugegoda, Sri Lanka

<sup>d</sup> Department of Physical Science, Trincomalee Campus, Eastern University of Sri Lanka, Nilaveli, Sri Lanka

<sup>e</sup> Department of Physics, University of Jaffna, Jaffna, Sri Lanka

<sup>f</sup> Department of Physics, University of Peradeniya, Peradeniya, Sri Lanka

## ARTICLE INFO

### Keywords:

Cadmium sulfide  
Chemical bath deposition  
Optical transmission  
Energy band gap  
Photoconductivity  
Grain size

## ABSTRACT

This paper presents a comprehensive study of the optical transmission, photoconductivity, and morphology of CdS thin films deposited via the chemical bath deposition (CBD) method. The films deposited for 60 min exhibit an optical energy band gap value of 2.42 eV and the highest optical transmission of 75 % in the wavelength range of 500–900 nm. For these films, the transmission electron microscopy imaging shows a distribution of particle sizes around 10 nm. The wavelength dependence of the photoconductivity, extracted from photo resistivity data, shows that the maximum photoconductivity occurs at 492 nm wavelength. This corresponds to an electrical energy band gap of 2.52 eV, which is greater than the optically measured energy gap of 2.42 eV. Based on these results, the electron-hole pair binding energy for CdS films is estimated as 100 meV. According to the electrical resistivity vs. temperature measurements, the activation energy is 1.26 eV which agrees with the electrical energy band gap of 2.52 eV. CdS films annealed under nitrogen gas at 200 °C for one hour exhibited an energy gap of 2.32 eV. These films displayed a conductivity of  $60 \times 10^{-4} \text{ Scm}^{-1}$ , a carrier concentration of  $6.38 \times 10^{14} \text{ cm}^{-3}$ , and a mobility of  $7.46 \text{ cm}^2 \text{ V}^{-1} \text{ s}^{-1}$ . These impressive characteristics suggest the suitability of CBD-grown CdS films annealed at 200 °C in nitrogen gas, to be used as the window material in CdS/CdTe thin film solar cells and other optoelectronic applications.

## 1. Introduction

It is well known that the estimated reserves of fossil fuels are insufficient to meet the growing global energy demand in the coming decades. The combustion of fossil fuels not only contributes to global warming through the emission of greenhouse gases but also poses health risks due to atmospheric pollution caused by particulate matter and toxic gases. The development of renewable energy sources, such as hydro, solar, and wind power, etc., offers a solution to these challenges by providing a sustainable and environmentally friendly energy supply to the world [1,2].

Among the various technologies available for harnessing renewable energy sources, solar photovoltaics stands out as a significant technology currently under development [3]. For several decades, the first

generation of solar cells based on semiconductor silicon has dominated the market. However, the intricate technology involved and the high manufacturing costs have hindered the widespread adoption of silicon solar panels for electricity generation. The second generation of solar cells, which includes three main thin-film photovoltaic technologies, has emerged as a viable alternative. These technologies are hydrogenated amorphous silicon (a-Si:H), cadmium telluride (CdTe), and copper indium gallium diselenide ( $\text{CuIn}_x\text{Ga}_{1-x}\text{Se}_2$ , or CIGS)[4].

Among the various options available, CdS is a highly intriguing semiconductor material due to its versatility in applications spanning optoelectronics, photovoltaics, catalysis, and biological sensing [5]. As an IIB-VIA semiconductor, CdS exhibits exceptional structural, electrical, and optical properties, making it a promising candidate for use as a buffer layer in a wide range of thin-film solar cells, including

\* Corresponding author at: National Institute of Fundamental Studies, Kandy, Sri Lanka.

E-mail address: [lakshman.di@nifs.ac.lk](mailto:lakshman.di@nifs.ac.lk) (M.A.K.L. Dissanayake).

<https://doi.org/10.1016/j.tsf.2024.140225>

Received 11 August 2023; Received in revised form 18 January 2024; Accepted 19 January 2024

Available online 22 January 2024

0040-6090/© 2024 Elsevier B.V. All rights reserved.

CdS/CuInSe<sub>2</sub> [6], CdS/CdTe [7], CdS/CuS [8], and more recently, Cu<sub>2</sub>ZnSnS<sub>4</sub>/CdS [9]. Furthermore, CdS finds utility in photodetectors, gas sensors, optical filters, thin film transistors, semiconductor lasers, and photoelectrochemical solar cells [10–13].

Several experimental techniques have been employed for the deposition of CdS thin films, including thermal evaporation, sputtering, spray pyrolysis, electrodeposition, pulsed laser deposition, and chemical bath deposition (CBD) [14–17]. Among these, CBD is widely favored for its simplicity, cost-effectiveness, and ease of reproducibility and use. In the CBD process, CdS films are grown on a microscopy glass substrate or a conductive glass substrate immersed in a chemical bath containing metallic ions (Cd<sup>2+</sup>) and chalcogen ions (S<sup>2-</sup>). A complexing agent (typically a base) is added to the bath to prevent the hydrolysis of the metallic ions. The controlled release of S<sup>2-</sup> ions within the solution facilitates the formation of CdS at low concentrations from the free Cd<sup>2+</sup> ions. The deposition of a uniform CdS film on the substrate occurs when the ionic product [Cd<sup>2+</sup>][S<sup>2-</sup>] exceeds the solubility product  $K_{sp} = 10^{-28}$ . Commonly used Cd sources include cadmium sulfate, cadmium acetate, cadmium chloride, and cadmium nitrate, while ammonia, ethylenediaminetetraacetic acid (EDTA), and triethanolamine are employed as complexing agents for cadmium ions. Sulfur sources agents such as thiourea, sodium sulfide, sodium thiosulfate, and thioacetamide have been utilized [16,17]. In this study, we focus on the fabrication of cadmium sulfide (CdS) thin films by CBD method, using cadmium chloride as the Cd source and ammonia as the complexing agent.

Although numerous studies have focused on the optical properties of CdS thin films prepared by CBD, only a few have explored some of the physical properties mentioned in our abstract, which are crucial, especially when considering the utilization of these films as window layers in CdS/CdTe solar cells and other optoelectronic devices. In this work, CdS thin films were prepared via CBD on three distinct glass substrates: microscopy glass, indium tin oxide (ITO) glass, and fluorine-doped tin oxide (FTO) glass. Subsequently, the CdS films were subjected to specific annealing conditions, and their structural, optical, electrical, and morphological properties were thoroughly examined. In particular, the study of the wavelength dependence of photoconductivity of CBD-grown CdS thin films was used to estimate the electrical energy bandgap of CdS thin films. This research is expected to contribute to optimizing the CBD-grown CdS films with respect to their optical and electrical properties to be used for the fabrication of CdS/CdTe solar cells, IR detectors, and other optoelectronic devices.

## 2. Experimental

### 2.1. Deposition of thin CdS films on microscopy glass, ITO, and FTO substrates by CBD method

In the present study, the CBD method was used to deposit visually homogeneous CdS thin films on three different substrates, namely commercial microscopy glass plates with dimensions 7.6 cm × 2.5 cm × 1.2 mm, FTO glass plates (~10 Ω/sq, Sigma-Aldrich, USA) of size 1.0 cm × 1.0 cm × 3 mm and ITO glass plates (~8–12 Ω/sq, Sigma-Aldrich, USA) of size 1.0 cm × 1.0 cm × 3 mm. The specific chemicals employed in the deposition process are detailed in Table 1. The substrates were first cleaned by the standard procedure by using a detergent, dilute HCl acid, de-ionized water, followed by ultrasound sonication and finally cleaned

**Table 1**  
Details of the chemicals used for the deposition of CdS thin film by CBD method.

Chemical	Amount of chemical	Purpose
De-ionized water	225 ml	Medium
Cadmium chloride	30 ml of 0.0405 M CdCl <sub>2</sub>	Cadmium source
Ammonium chloride	10 ml of 0.643 M NH <sub>4</sub> Cl	pH buffer
Thiourea	30 ml of 0.2036 M thiourea	sulfur source
Ammonium hydroxide	15 ml of 1.0 M NH <sub>4</sub> (OH)	pH control

with an organic solvent. The precursor solution was prepared as follows. First, 225 ml of de-ionized water in a 300 ml beaker was heated to a temperature of around 70 °C while being stirred using a magnetic stirrer. Once the bath temperature reached 70 °C, the following chemicals were sequentially added into the water bath: 30 ml of 0.0405 M CdCl<sub>2</sub> (98 %, Sigma-Aldrich, USA), 10 ml of 0.643 M of NH<sub>4</sub>Cl (98 %, Sigma-Aldrich, USA), and 30 ml of 0.2036 M of thiourea (CS(NH<sub>2</sub>)<sub>2</sub> 99 %, Sigma-Aldrich, USA). Then the addition of NH<sub>4</sub>OH (1 M, Sigma Aldrich, USA) to the above solution mixture was performed using the titration method, while continuously stirring until a noticeable color change to yellow was observed. This point was reached when the volume of NH<sub>4</sub>OH (1 M) was around 15 ml. Throughout this deposition, the solution bath was continuously stirred using a magnetic stirrer and was maintained at a temperature of 65 °C and a pH of 10. The substrates were removed from the bath one-by-one at intervals of 10 min, up to a total deposition time of 60 min in order to vary the film thickness by varying the deposition times to 20, 30, 40, 50, and 60 min respectively. Subsequently, CdS-coated substrates were rinsed with deionized water, and the CdS layers on the backside of the substrates were carefully removed using HCl. In order to check the reproducibility of different characterizations for as-deposited CdS films of different thicknesses, the entire CBD process was repeated five times with new substrates and new precursor solutions.

### 2.2. Annealing of CdS films

Annealing is a commonly employed process aimed at reducing lattice stress, improving mismatch, and promoting interdiffusion between elements at the interface of deposited CdS films. In this study, CdS thin films, which had been deposited on microscopy glass substrates using the CBD method were subjected to an annealing process. The films were annealed in a nitrogen (N<sub>2</sub>) environment at two different temperatures 100 °C and 200 °C, each for a duration of 30 min while continuously purging nitrogen gas to ensure that oxygen is not present. For this purpose, a quartz tube furnace equipped with a temperature controller and gas flow controls at the inlet and outlet for N<sub>2</sub> flow was used. The effect of annealing was visually observable by the color changes in the films: the as-deposited films exhibited a light-yellow appearance, while the annealed films appeared orange.

### 2.3. Measurement of optical absorbance spectra of as-deposited and annealed CdS films

UV–vis absorbance spectra were taken for the as-deposited CdS thin films prepared using the CBD method and subsequently annealed, as described earlier. For this purpose, a UV–vis 2450 (SHIMADZU) spectrophotometer was employed in the wavelength range from 190 nm to 1100 nm. To determine the energy band gap ( $E_g$ ) values, a plot of (Absorbance × Photon Energy)<sup>2</sup> against Photon Energy was used (please see Section 3.1).

### 2.4. Photoconductivity of CdS films

To investigate the variation in photoconductivity with incident wavelength for the CdS films deposited on microscopy glass substrates for one-hour, the sheet resistance values of as-deposited films were measured by the Van Der Pauw Method using a Keithley source meter (Model 2601). Subsequently, the resistance vs wavelength variation was converted to the photoconductivity vs wavelength variation. In this experiment, the wavelength of incident light was varied using a monochromator. As the intention of this study was to determine the wavelength that corresponds to the conductivity maximum, the thickness of the CdS film was not measured.

## 2.5. Four-probe electrical conductivity measurements

In order to measure the electrical conductivity of the as-deposited CdS films, a four-point probe setup consisting of four tungsten metal tips with finite radius, equally spaced with a typical probe spacing of approximately 2 mm, was utilized. To minimize any potential damage to the sample during measurements, each tip was supported by springs at the end. A high-impedance current source (Keithley Model 2601 Source meter) was employed to supply current through the outer two probes, while a digital voltmeter was used to measure the voltage across the inner two probes, enabling the determination of the sample resistivity. Specifically, a small current ( $I$ ) of the order of 50 mA was directed through the outer two probes from the constant current source, and the voltage ( $V$ ) was measured between the inner two probes. These measurements were conducted while varying the temperature of the CdS sample. The energy band gap of the CdS semiconductor film was then calculated using the gradient of the resulting  $\ln \frac{V}{I}$  vs  $\frac{1000}{T}$  graph.

## 2.6. Hall effect measurements

The conductivity type and carrier concentration in CdS were determined by using the Hall Effect apparatus (PHYWE Systeme GmbH & Co. KG, Germany). The resistivity and Hall voltage of a rectangular as-deposited CdS film sample formed of microscopy glass was measured as a function of temperature and magnetic field. The specific conductivity, the type of charge carriers and the mobility and the concentration of the charge carriers were determined from the measurements. In this setup, a CBD-CdS film deposited on a thin glass slide was subjected to a magnetic field perpendicular to the film. Hall voltage was measured by varying the current through the film. The carrier concentration was determined from the gradient of the graph of the Hall voltage vs current passed through the film.

## 3. Results and discussion

### 3.1. Optical properties of CdS thin films deposited by chemical bath deposition method

The UV-vis optical absorbance spectra ( $A$ ) of CdS thin films as-deposited on microscopic glasses for different deposition times in the wavelength range of 300–900 nm were converted to the absorption coefficient  $\alpha$  using Eq. (1) and corresponding film thicknesses (Table 2) and are shown in Fig. 1. For clarity, we are presenting here only one set of Absorption coefficient vs Wavelength values for each film thickness (each deposition time), even though we have taken these measurements and performed the analysis for five independent depositions for each time period.

As seen from this figure, the absorption coefficient values increase with increasing film thickness, as expected according to Beer Lambert's law. Yakuphanoglu et al. [18], Nada et al. [19], and several others have reported similar results. As the thickness of CdS films increases, the particle size of CdS also increases, and the corresponding optical absorption edge decreases (Table 2). This is also associated with a decrease

**Table 2**

Variation of energy band gap values and particle sizes estimated based on them for as-deposited CdS thin films with different thicknesses formed on microscopy glass substrates.

Sample label	Deposition time (minutes)	Film Thickness (nm)	Energy band gap $E_g$ (eV)	Estimated Particle size (nm)
A	20	46.0 ± 0.1	2.52 ± 0.02	6.07
B	30	69.4 ± 0.1	2.47 ± 0.02	7.11
C	40	92.0 ± 0.1	2.44 ± 0.03	8.15
D	50	115.2 ± 0.1	2.43 ± 0.03	8.64
E	60	138.0 ± 0.1	2.42 ± 0.03	9.27

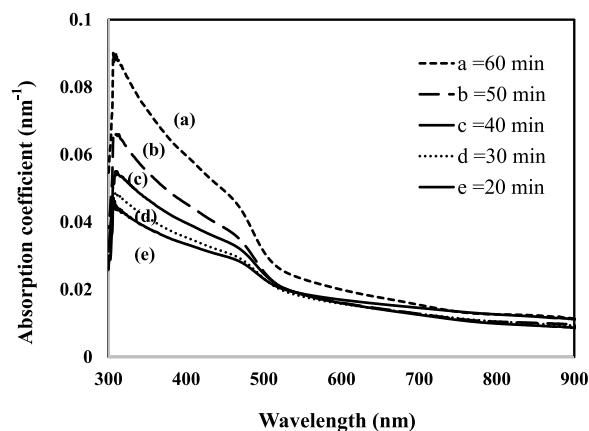


**Fig. 1.** UV-vis absorption coefficient vs wavelength of as-deposited CdS film of different thicknesses deposited on microscopy glass substrates by CBD method.

in defect concentration and resistivity and an increase in mobility [19, 20]. These findings are important for preparing CdS thin films for the fabrication of CdS/CdTe solar cells and other optoelectronic detectors.

Experimentally, the absorption coefficient ( $\alpha$ ) can be calculated from this simple relation:

$$\alpha = 1/t \ln [(1 - R)^2 / T]$$

where  $t$  is the sample thickness, and  $T$  and  $R$  are the transmission and reflection coefficients. However, since we have determined the optical absorbance  $A$  and not the  $T$  and  $R$  values, we can use the relation,

$$\text{Absorption coefficient } (\alpha) = 2.303 A / t \quad (1)$$

where ( $A$ ) is the absorbance and ( $t$ ) is the thickness of the thin film. For a given sample, since the thickness is a constant, we can write, that the absorption coefficient is proportional to the absorbance. Following this, near the absorption edge, the following Tauc Relation (1) can be used to determine the energy band gap  $E_g$  of CdS.

$$(ah\nu)^2 = C(h\nu - E_g)^n \quad (2)$$

where  $h\nu$  is the incident photon energy,  $\alpha$  is the optical absorption coefficient,  $C$  is a constant,  $h$  is the Planck's constant and  $n$  is equal to 1 for direct band gap materials such as CdS.

Fig. 2 was obtained by plotting  $(ah\nu)^2$  versus photon energy ( $h\nu$ ) graph for as-deposited CdS films deposited with different deposition times on microscopic glass substrates. The extrapolated, best tangent, straight lines were used to determine the intersection on the photon energy axis, to extract the energy band gap  $E_g$  values. A similar procedure has been followed by many previous workers to determine the energy band gap value of CdS films from optical absorbance data [20–26].

The energy band gap values obtained from Fig. 2 are 2.52, 2.47, 2.44, 2.43 and 2.42 eV for the CdS films deposited for 20, 30, 40, 50, and 60 min respectively. Each of these values represent the average value obtained from five independent depositions for each time duration. Tauc plots for the films deposited for 20 and 30-min durations give energy band values within  $\pm 0.02$  eV while for the next three deposition times, 40, 50 and 60 min, the energy band values were within  $\pm 0.03$  eV. From these results, it is clear that the energy band gap values decrease with increasing deposition time and increasing film thickness along with increasing particle size (See Table 2). Similar behavior has been reported by Nada et al. [19], Jafari et al. [21], and Flores et al. [22] from their studies. Out of these CdS films, the films that were deposited for 60 min can be selected as suitable for fabricating the CdS/CdTe solar cells as they give the actual energy band gap value of 2.42 eV, which corresponds to the bulk CdS [23–26].

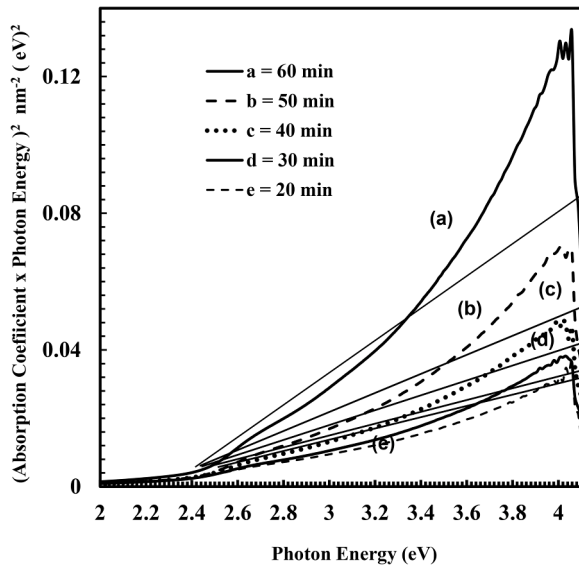


Fig. 2. (Absorption Coefficient  $\times$  Photon Energy)<sup>2</sup> vs Photon Energy ( $h\nu$ ) graph for different thicknesses of as-deposited CdS films on microscopy glass substrate by CBD method.

As obtained from Fig. 2, the value of the as-deposited CdS films on a microscope glass substrate for 60 min is 2.42 eV ( $\pm 0.03$  eV). This  $E_g$  value is in good agreement with the values reported by Flores et al. [22], Jafari et al. [21], and Raji et al. [27] for the actual energy band gap values of the CdS bulk material. Therefore, CdS films deposited for 60 min were used for further studies.

### 3.2. Estimate of the CdS particle size from UV–vis absorption spectra

The particle size of CBD-deposited CdS films can be estimated from the UV–vis absorption spectra using the following expression derived from the effective mass model [28]. According to the effective mass approximation model, the band gap of semiconductor nanoparticles (considered as a sphere with radius  $r$ ) is given by:

$$E_g^* = E_g^{\text{bulk}} + \frac{\hbar^2 \pi^2}{2r^2} \left( \frac{1}{m_c^*} + \frac{1}{m_h^*} \right) - \frac{1.8e^2}{4\pi\epsilon\epsilon_0 r} - \frac{0.124e^4}{\hbar^2 (4\pi\epsilon\epsilon_0)^2} \left( \frac{1}{m_c^*} + \frac{1}{m_h^*} \right)^{-1} \quad (2a)$$

where,  $E_g^*$  is the energy band gap of the CdS nanoparticle, corresponding to the UV–vis absorbance spectrum,  $E_g^{\text{bulk}}$  is the energy band gap of the bulk CdS at room temperature,  $\hbar = \frac{h}{2\pi}$  is the Planck's constant,  $r$  is the radius of the particle, and  $m_c^* = 0.19 m_e$  and  $m_h^* = 0.80 m_e$  are the effective masses of conduction band electron and valance band hole in CdS thin film as reported by Lippens et al. based on a band structure calculation for CdS [29].

The first term in the above effective mass model equation represents the kinetic energy term, which shifts the  $E_g^*$  to higher energies proportional to  $1/r^2$ . The second term arises due to the screened coulomb interaction between the electron and hole, and it shifts the  $E_g^*$  to lower energy as  $1/r$ . The third, size-independent term, is the solvation energy loss which is usually small and can be ignored.

Table 2 shows the relation between the energy band gap values, film thickness and particle sizes of as-deposited CdS thin films using the CBD method on microscopy glass substrates. The energy band gap decreases, and the particle size increases with the deposition time. Similar results were reported by Nada et al. [19], Mane et al. [30] and Srinivasa et al. [31]. These observations are in agreement with the quantum confinement effect. The thicknesses of the as-deposited CdS films were measured by an Optical Profilometer and the thickness of the film from 60 min deposition time is 138.0 nm. As seen from the above Table, the

estimated particle sizes of as-deposited CdS films on microscopy glass substrate for 60 min is 9.27 nm.

The Transmission Electron Microscopy (TEM) image of CdS particles taken from as deposited CdS film on microscopy glass substrate for 60 min is shown in Fig. 3. The CdS particles seen in the TEM image show a distribution of sizes, ranging from 9.5 nm to 12.4 nm. According to Han et al. the TEM image of CBD-CdS films consist of particles in the 5–10 nm range [32].

Fig. 4 shows the UV–vis absorbance and transmission spectra of CdS thin films as-deposited on microscopy glass substrate by CBD method for 60 min. All subsequent experiments were also performed using the CdS films deposited for 60 min. The optical absorbance and transmission spectra can be analyzed considering two wavelength regions, 300–500 nm and (b) 500–900 nm. In region (a), the films exhibit low optical transmission and high optical absorbance behavior. Similar results have been reported by Hasnat et al. [33] and Osuwa et al. [34]. In region (b) the films exhibit more than 75 % transmission. The transmission is very low in the region (a) because of incident light of higher photon energy compared to the energy band gap of CdS films (2.42 eV). In a CdS/CdTe thin film solar cell, CdS thin film acts as the window layer so that it should have a high transmission in the absorption wavelength range of the CdTe layer. Therefore, the CdS thin films deposited by CBD for 60 min in this work appear to be the most appropriate for fabricating CdS/CdTe thin film solar cells.

### 3.3. Photoconductivity and electrical energy band gap of CdS films

The photoconductivity vs wavelength variation depicted in Fig. 5 was extracted from the measured sheet resistance vs the wavelength of the incident light data for the CdS samples as-prepared by CBD for 60 min. The CdS film thickness, as measured by the optical profilometer, was 138 nm. However, as mentioned before, for this study, the absolute value of the sheet resistance was not needed as the main interest was only in the wavelength that corresponds to the minimum of the sheet resistance or the maximum of the photoconductivity. For this reason, the y-axis has been marked in arbitrary units.

According to Fig. 5 initially, the photoconductivity increases sharply with the wavelength exhibiting a short wavelength tail, raising to a peak at 492 nm and then falling off rapidly at first and then more slowly towards longer wavelengths. Park et al. [35], Mahdi et al. [36], and John et al. [37] also observed the variation of photocurrent with the wavelength of incident light for CdS single crystals with a similar trend, but the peak maximum occurs at a slightly different wavelength. Mahdi et al. [36] used CdS single-crystalline photodetector and observed the photoconductivity of the fabricated Al/CdS single-rod device with a photoconductivity peak at 480 nm. In our case, for the CBD grown CdS films, the wavelength of 492 nm where the photoconductivity maximum of occurs corresponds to an electrical energy band gap of 2.52 eV. It should be noted that this value is greater than the optically measured energy band gap of 2.42 eV for the 60 min as-deposited films. From a study of the spectral response of CdS single-crystal nanoribbons, Jie et al. [38] has reported that as the wavelength of incident light increases, the photoconductivity increases steeply and reaches a maximum at 490–495 nm. Following these authors, we can attribute the photoconductivity in CBD grown CdS films also to the electron-hole pair excitation by the incident light with energy larger than the optical band gap; i.e., only light with enough photon energy is able to form excitons (electron-hole bound pairs) by exciting electrons from the valence band to the conduction band and thus contributing to the photocurrent.

As can be seen from Fig. 5, beyond the maximum at 492 nm, the photoconductivity values of as-deposited CdS thin film first decrease with the increasing wavelength in the range between 500 nm and 650 nm, and after that, from 650 to 900 nm it becomes almost constant. Therefore, it can be concluded that the optical absorption of CdS films beyond 650 nm is minimum while the optical transmission beyond 650 nm is maximum, in general agreement with optical absorption/

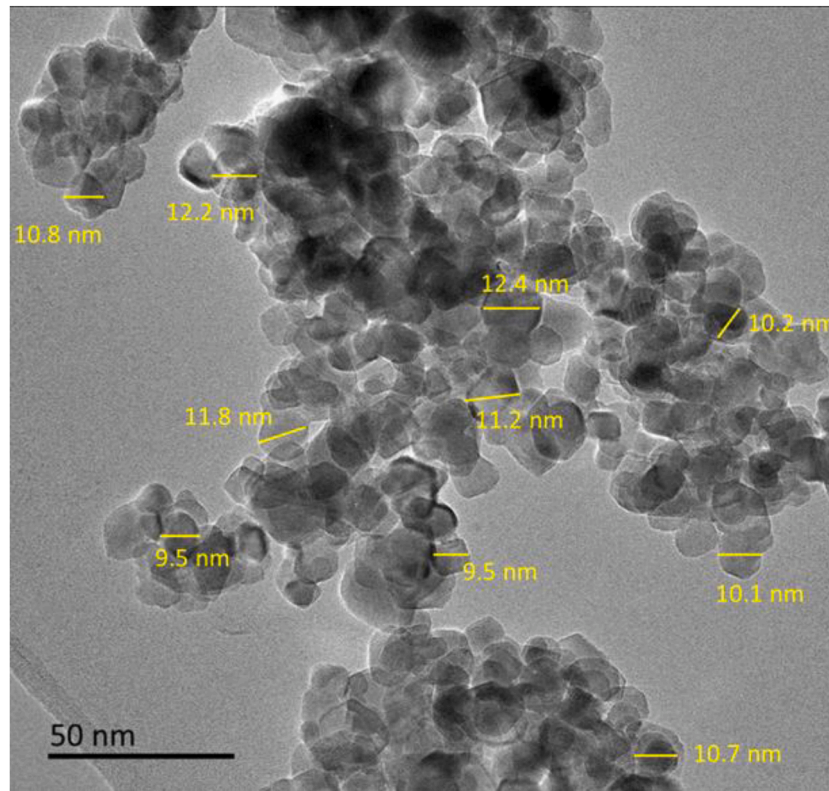


**Fig. 3.** The TEM image of a CdS film as-deposited on microscopy glass substrate for 60 min showing the range particle sizes.

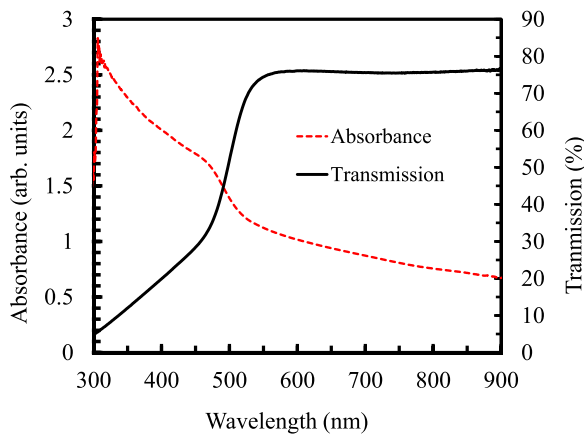


**Fig. 4.** UV-vis absorbance and transmission spectra of CdS thin films as-deposited on microscopy glass substrate by CBD method for 60 min.

transmissions results shown in Fig. 4. This confirms the suitability of CdS films as the window layer in CdS/CdTe solar cells. All previous reports on photoconductivity vs wavelength are based on results taken for CdS single crystals. Even in reports on photoluminescence (PL) studies of CdS thin films, the electrical energy band gap has not been discussed [39, 40]. This report covers the photoconductivity vs wavelength study made on CBD-grown CdS films of thickness 138 nm.

CdS is an n-type, II-VI semiconductor with a direct band gap of 2.42 eV at room temperature. This corresponds to a maximum optical absorption peak at 514 nm wavelength which shows that CdS can absorb visible light and UV light up to 514 nm (see Figs. 2 and 4). In a semiconductor material, the optical bandgap ( $E_{opt}$ ) is the threshold for photons to be absorbed by creating an exciton (bound electron-hole pair), while the electrical band gap ( $E_{el}$ ) is defined as the threshold for

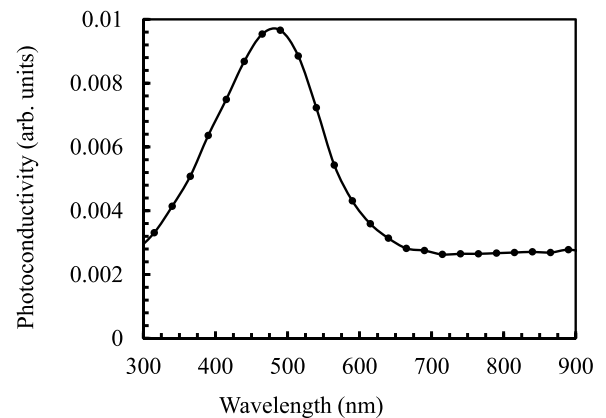


**Fig. 5.** Photoconductivity variation with the wavelength of incident light for a CdS thin film as-deposited on microscopy glass substrate by CBD method for 60 min. Photoconductivity maximum occurs at 492 nm wavelength.

separating the electron-hole pair. The optical bandgap is at a lower energy than the electrical bandgap. The difference  $E_{el} - E_{opt}$  corresponds to the electron-hole pair binding energy. When a conduction band electron drops down to recombine with a valence band hole, both are annihilated, and energy is released as a light photon (Fig. 6). This is the principle of the light-emitting diode or LED. While the optical band gap measurement is important for applications such as solar cells, the electrical band gap measurement is important for optoelectronic devices such as light-emitting diodes and laser diodes [41].

In the present study, for as-deposited CdS films, we have obtained the optical energy bandgap,  $E_{opt} = 2.42$  eV from optical absorption measurements, (Fig. 1) and  $E_{el} = 2.52$  eV from photoconductivity data. Therefore,  $E_{el} - E_{opt} = 0.10$  eV = 100 meV which gives an estimate of the electron-hole pair binding energy in CBD grown CdS films.

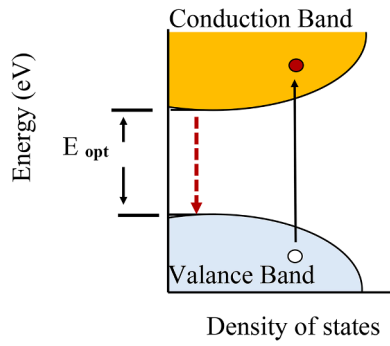


**Fig. 6.** An electron-hole pair is created when light energy  $E > E_{\text{gap}} = E_{\text{opt}}$  is absorbed by a semiconductor (the up-arrow). When the electron-hole pair recombines it releases energy equal to  $E_{\text{gap}} = E_{\text{opt}} = 2.42$  eV (the down- arrow). In the present case,  $E_{\text{opt}} = 2.42$  eV, and  $E_{\text{elect}} = 2.52$  eV for as-deposited CdS films.

**3.4. Temperature dependence of electrical resistivity of CdS films**

In order to determine the activation energy associated with electrical resistivity for the as-deposited CdS thin films, the four-probe electrical conductivity measurement were performed as described in Section 2.6. Resistivity of the intrinsic semiconductor at high temperature can be expressed in the following form,

$$\rho = \rho_0 \exp\left(\frac{E_a}{kT}\right) \tag{3}$$

where  $\rho$  is the resistivity of the sample at temperature  $T$ ,  $\rho_0$  is the resistivity of the sample at room temperature,  $E_a$  is the activation energy,  $k$  is the Boltzmann constant. By using the equation for the resistivity as

$$\rho = \frac{Rl}{A} = \frac{VI}{IA} \tag{4}$$

where, resistance  $R = \frac{V}{I}$ , and  $V$  and  $I$  are the voltage and current across the inner two probes.

$l$  and  $A$  are the length and cross-section area of the samples, which are constants. By rearranging Eq. (3) as;

$$\ln \frac{V}{I} = \frac{E_a}{1000k} \frac{1000}{T} + C \tag{5}$$

a liner equation of the form  $y = mx + c$  can be obtained.

Fig. 7 shows the  $\ln \frac{V}{I}$  vs  $\frac{1000}{T}$  graph for CdS thin film on microscopic glass, measured in the temperature range of from 150 to 200 °C. From

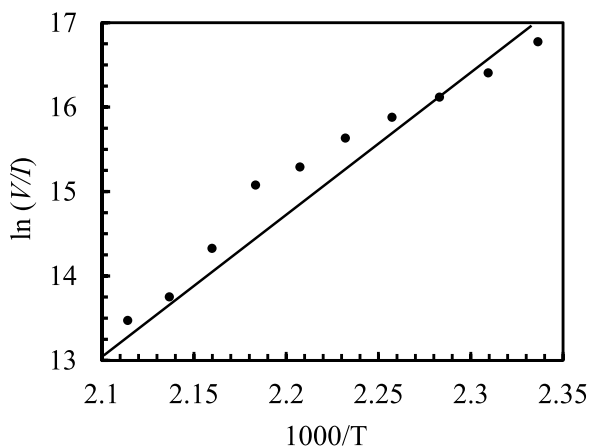


**Fig. 7.** Plot of  $(V/I)$  vs  $1000/T$  for as-deposited CdS thin film formed on microscopy glass slide (60 min).

the slope of  $[\ln \frac{V}{I}$  vs  $\frac{1000}{T}]$ , the electrical energy band gap of the material can be calculated as  $E_g = 2E_a$ .

The activation energy calculated from the linear graph in Fig. 7 is  $E_a = 1.26$  eV. Therefore, the estimated electrical energy gap,  $E_{\text{elect}} = 2E_a = 2.52$  eV, generally agrees with the maximum of the photoconductivity vs wavelength graph (Fig. 5).

**3.5. Estimation of carrier concentration of CdS films**

To further characterize the CBD-grown CdS films, the results of the Hall Effect measurements were used and the carrier concentration and carrier mobility of the as-deposited CdS thin films on glass substrates by CBD method were estimated. As determined from the direction of the Hall voltage, the carrier type is found to be of  $n$ - type. The carrier concentrations ( $n$ ) of the thin CdS films is related to the Hall voltage by,

$$V_H = \frac{IBw}{nAe} = \frac{B}{nte}I \tag{6}$$

where,  $q = e$  is the charge of the electron,  $B$  is the magnetic field applied perpendicular to the semiconductor,  $w = 0.8$  cm is the width of the specimen,  $t$  is the thickness of the specimen,  $I = nAve$  is current through the specimen and  $n$  is charge carrier concentration. The estimated value of conductivity of the specimen is given by  $\sigma = ne\mu = \frac{1}{\rho}$ , where  $\mu$  is the mobility of the specimen, and  $\rho$  is the resistivity of the sample given by  $\rho = \frac{Rwt}{l}$ , where  $R$  is the resistance ( $R = \frac{V}{I}$ ) of the sample. Then,  $\sigma = \frac{1}{\rho} = \frac{l}{Rwt}$  and the mobility of the specimen is given by  $\mu = \frac{\sigma}{ne}$ .

As measured by the optical profilometer, the average thickness of the as-deposited CdS films on microscopy glass substrate for 60 min was  $t = 138.0$  nm ( $\pm 0.1$  nm).

Table 3 shows the estimated values of the conductivity, carrier concentration and carrier mobility of the CdS thin films fabricated on glass substrates. These values are comparable with the values reported by Hani et al. [42], Fahrenbruch et al. [43], Nazr et al. [44] and Gopi et al. [45]. Resistivity, conductivity, carrier concentration and mobility of as-deposited CdS films on glass substrate obtained in this work and shown in Table 2 are  $1.31 \times 10^3 \Omega \text{ cm}$ ,  $7.6 \times 10^{-4} \text{ S cm}^{-1}$ ,  $6.38 \times 10^{14} \text{ cm}^{-3}$  and  $7.46 \text{ cm}^2 \text{ V}^{-1} \text{ s}^{-1}$  respectively. These results are generally in agreement with those reported by previous workers. It should be noted that, in order to achieve maximum power conversion efficiency in CdS/CdTe thin film solar cells it is necessary to have a window material made with a semiconductor with low resistivity which allows effective and easy separation of electrons and holes upon incident light [43]. Based on these values and optical properties, we can suggest that the CdS films prepared by the CBD method and annealed at 60 °C in  $N_2$  are suitable to be used as window materials in CdS/CdTe hetro junction solar cells.

**Table 3**  
Comparison of electrical properties of as-deposited CdS thin films formed on microscopy glass substrate by CBD method.

Sample name	Resistivity ( $\Omega\text{cm}$ )	Conductivity ( $\text{Scm}^{-1}$ )	Carrier concentration $n$ ( $\text{cm}^{-3}$ )	Mobility ( $\text{cm}^2\text{V}^{-1}\text{s}^{-1}$ )
This work (CdS / glass)	$1.31 \times 10^3$	$7.60 \times 10^{-4}$	$6.38 \times 10^{14}$	7.46
Reference [33] 2008	$2.96 \times 10^3$	—	$9.74 \times 10^{14}$	1.96
Reference [34] 1983	—	$10^{-8}$ to $10^2$	—	1 to $10^5$
Reference [35] 2013	$2.44 \times 10^3$	—	$2.48 \times 10^{15}$	3.16
Reference [36] 2023	$2.8 \times 10^2$	—	$4.4 \times 10^{15}$	5.0

### 3.6. Effect of annealing on optical properties of CdS films

As shown in Fig. 4 for the CdS film deposited for 60 min, the optical absorbance spectrum and the transmission spectrum are complementary to each other. As optical absorbance is the most widely used parameter for the characterization of thin semiconductor films, in this work, we have used the absorbance spectra instead of the transmission spectra for determining the energy band gap values. Table 4 shows the dependence of the energy band gap values of CBD-grown CdS films deposited on the three different substrates for 60 min on the annealing temperature, as determined from optical absorbance vs photon energy graphs (not shown).

According to Table 3, the energy band gap of as-deposited CdS thin films prepared on microscopy glass substrates is 2.42 eV, while the energy bandgap of films annealed at 100 and 200 °C in N<sub>2</sub> atmosphere are 2.39 and 2.32 eV respectively. A similar decrease in the energy band gap value with annealing temperature can be observed for CdS films deposited in FTO and ITO substrates. These observations are in general agreement with results reported by Ichimura et al. [45], Metin et al. [46], and Elmas et al. [47], also in agreement with observations reported by Mustafa et al. [48], Ichimura et al. [46], Metin et al. [47], Elmas et al. [48], and Yu et al. [49]. The possibility of oxidation of the CdS sample during annealing can be ruled out as the annealing was done in a tube furnace continuously purged with nitrogen gas. The average thickness of the CdS films as measured by the optical profilometer is 138 nm for the as-deposited films and 115 nm for the films annealed under N<sub>2</sub> gas at 200 °C for one hour.

Based on their recent (2023) work, Gopi et al. [45] have reported that the solar cells made with as-deposited CdS exhibit the lowest photon conversion efficiency (PCE), whereas the devices made with 200 °C vacuum and air-annealed CdS buffer layer resulted in the solar cells with the best PCE. For the CdS/CdTe solar cells made with as-deposited CdS, this effect has been related to the surface morphology of the CdS layer, containing smaller grains which significantly reduces the formation of the favorable heterojunction interface between CdS and CdTe resulting in reduced PCE of the corresponding solar cell. On the other hand, for the device made with CdS annealed at 200 °C, the formation of better CdS/CdTe interface is facilitated due to the formation of larger CdS grains and a more dense film with less grain boundaries which has led to higher PCE cells. According to this report, by annealing the sample at 200 °C the band gap of CdS decreased from 2.42 to 2.32 eV and the electron density dropped from  $\sim 10^{18}$  to  $\sim 10^{11}$  cm<sup>-3</sup>. As deposited CdS films have shown n-type conductivity with  $4.4 \times 10^{15}$  cm<sup>-3</sup> carrier concentration,  $5$  cm<sup>2</sup> V<sup>-1</sup> s<sup>-1</sup> mobility, and  $2.8 \times 10^2$  Ω cm resistivity. The energy band gap of CdS films deposited on glass substrates was determined from a Tauc plot based on the UV-vis measurements, and it was found that, as deposited CdS, films have exhibited a band gap value of 2.42 eV, similar to ours. As the annealing temperature in air was increased to 400 °C, a clear trend of band gap decrease has been observed.

According to Quinonez-Urias et al. [50], carrier mobility is inversely proportional to the film roughness, and carrier concentration is proportional to the grain size. Therefore, due to the annealing process, the carrier mobility and carrier concentration are also expected to increase, leading to an increase in the short-circuit current density,  $J_{sc}$  of the solar cell, enhancing its efficiency. In summary, a denser CdS layer with larger grains, lower surface roughness, higher carrier concentration and higher mobility, resulting from improved interfacial heterojunction between the n-CdS and p-CdTe layers would lead to the reported higher PCEs fabricated with annealed CdS films [51–60].

## 4. Conclusions

In this work, we have studied the optical and electrical properties of CBD-deposited CdS films and their morphology. The CdS films, as-deposited for 60 min by the CBD method, has a thickness of 138 nm

**Table 4**

The dependence of the energy bandgap values of CBD-grown CdS films deposited on different substrates on the annealing temperature. The energy values given here are within  $\pm 0.03$  eV.

Substrate	Before annealing (eV)	annealed in N <sub>2</sub> at 100 °C (eV)	annealed in N <sub>2</sub> at 200 °C (eV)
Glass	2.42	2.39	2.32
FTO	2.40	2.38	2.35
ITO	2.30	2.27	2.24

and exhibit an optical energy band gap of 2.42 eV. According to the TEM imaging the average particle size for these films is found to be around 10 nm. These CdS films also exhibit the highest optical transmission of 75 % in the wavelength range of 500–900 nm, which is ideally suitable for CdS/CdTe thin film solar cells. As an important finding from the present work, this paper reports the wavelength dependence of the photoconductivity of CdS thin films, and shows that the maximum photoconductivity occurs at 492 nm wavelength. This corresponds to an electrical energy band gap of 2.52 eV, which is greater than the optically measured energy gap of 2.42 eV. These results provide an estimate of the electron-hole pair binding energy as 110 meV for CdS films. Electrical resistivity vs. temperature measurements gives an activation energy of 1.265 eV, in agreement with the electrical energy band gap of 2.52 eV. Additionally, the annealed CdS films displayed a conductivity of  $7.60 \times 10^{-4}$  S cm<sup>-1</sup>, a carrier concentration of  $6.38 \times 10^{14}$  cm<sup>-3</sup>, and a mobility of  $7.46$  cm<sup>2</sup> V<sup>-1</sup> s<sup>-1</sup>. These impressive characteristics indicates the suitability of CBD grown CdS thin films annealed at 200 °C in N<sub>2</sub> gas, to be used as the window material in CdS/CdTe thin film solar cells and other optoelectronic applications [26,29,55].

### CRedit authorship contribution statement

**M.A.K.L. Dissanayake:** Project administration, Funding acquisition, Conceptualization. **K. Paramanathan:** Methodology, Investigation, Conceptualization. **G.K.R. Senadeera:** Writing – review & editing, Supervision, Formal analysis. **C.A. Thotawattage:** Methodology, Data curation. **K. Balashangar:** Validation, Investigation. **P. Ravirajan:** Project administration, Funding acquisition. **B.S. Dassanayake:** Project administration, Funding acquisition.

### Declaration of competing interest

The authors declare that they have no known competing financial interests or personal relationships that could have appeared to influence the work reported in this paper.

### Data availability

Data will be made available on request.

### Acknowledgments

Authors wish to thank the “Edu-Training project for prototype manufacturing of thin film solar cells” of the State Ministry of Skills Development, Vocational Education, Research & Innovations, Sri Lanka and the National Science Foundation (Research Grant: RG/2012/BS/04) for financial support and the National Institute of Fundamental Studies, Department of Physics, University of Peradeniya and Department of Physics, University of Jaffna, Sri Lanka. The experimental facilities provided by Sivananthan Laboratories, Bollingbrook, USA and the Microphysics Laboratory, University of Illinois at Chicago, USA are gratefully acknowledged.

*This paper is dedicated to the memory of our collaborator and co-author, DR. BUDDHIKA S. DASSANAYAKE, who tragically passed away on*

December 26, 2023.

## References

- [1] R.L. Ottinger, R. Williams, Renewable energy sources for development, *Environ. Law* 32 (2) (2002) 331–368. [www.jstor.org/stable/43267559](https://www.jstor.org/stable/43267559).
- [2] P.A. Owusu, S. Asumadu-Sarkodie, A review of renewable energy sources, sustainability issues and climate change mitigation, *Cogent Eng.* 3 (1) (2016) 1167990, <https://doi.org/10.1080/23311916.2016.1167990>.
- [3] W.C. Sinke, Development of photovoltaic technologies for global impact, *Renew. Energy* 138 (2019) 911–914.
- [4] T.D. Lee, A.U. Eboang, A review of thin film solar cell technologies and challenges, *Renew. Sustain. Energy Rev.* 70 (C) (2016) 1286–1297, <https://doi.org/10.1016/j.rser.2016.12.028>.
- [5] C.W. Wei, S.S. Hou, Preparation and optical properties of blue-emitting colloidal CdS nanocrystallines by the solvothermal process using poly (ethylene oxide) as the stabilizer, *Colloid Polym. Sci.* 285 (2007) 1343–1349.
- [6] K. Orgassa, U. Rau, Q. Nguyen, R.U. Osuji, P.U. Asogwa, Role of the CdS buffer layer as an active optical element in Cu(In,Ga)Se<sub>2</sub> thin-film solar cells, *Prog. Photovolt.* 10 (2002) 457–463.
- [7] H.N. Cui, S.Q. Xi, The fabrication of dipped CdS and sputtered ITO thin films for photovoltaic solar cells, *Thin Solid Films* 288 (1996) 325–329.
- [8] F.I. Ezema, D.D. Hile, S.C. Ezugwu, R. Osuji, Optical properties of CdS/CuS & CuS/CdS heterojunction thin films deposited by chemical bath deposition technique, *J. Ovon. Res.* 6 (2010) 99–104.
- [9] M. Courel, J.A. Andrade-Arzuvo, O. Vigil-Galán, Loss mechanisms influence on Cu<sub>2</sub>ZnSnS<sub>4</sub>/CdS-based thin film solar cell performance, *Solid-State Electron.* 111 (2015) 243–250.
- [10] A. Nazir, A. Toma, N.A. Shah, S. Panaro, S. Butt, R.R. Sagar, W. Raja, K. Rasool, A. Maqsood, Effect of Ag doping on opto-electrical properties of CdS thin films for solar cell application, *J. Alloys Compd.* 609 (2014) 40–45.
- [11] B. Pradhan, A.K. Sharma, A.K. Ray, Conduction studies on chemical bath-deposited nanocrystalline CdS thin films, *J. Cryst. Growth* 304 (2) (2007) 388–392.
- [12] X. Duan, Y. Huang, R. Agarwal, C.M. Lieber, Single-nanowire electrically driven lasers, *Nature* 421 (2003) 241–245.
- [13] W. Kim, M. Seol, H. Kim, et al., Freestanding CdS nanotube films as efficient photoanodes for photoelectrochemical cells, *J. Mater. Chem. A* 1 (2013) 9587–9589.
- [14] K. Senthil, D. Mangalaraj, R. Narayanadas, R. Kesavamoorthy, G.L.N. Reddy, B. Sundaravel, Implantation effects in vacuum evaporated CdS thin films using Raman scattering and X-ray diffraction studies, *Physica B* 304 (2001) 175–180.
- [15] D. Kim, Y. Park, M. Kim, Y. Choi, Y.S. Park, J. Lee, Optical and structural properties of sputtered CdS films for thin film solar cell applications, *Mater. Res. Bull.* 69 (2015) 78–83.
- [16] G. Hodes, *Chemical Solution Deposition of Semiconductor Films*, CRC Press, New York, 2002.
- [17] M. Cao, Y.M. Sun, J.J. Wu, X. Chen, N. Dai, Effects of cadmium salts on the structure, morphology and optical properties of acidic chemical bath deposited CdS thin films, *J. Alloys Compd.* 508 (2010) 297–300.
- [18] F. Yakuphanoglu, C. Viswanathan, P. Peranathan, D. Soundarrajan, Effects of the film thickness on optical constants of transparent CdS thin films deposited by chemical bath deposition, *J. Optoelectron. Adv. Mater.* 11 (7) (2009) 945–949.
- [19] K.A. Nada, K.A. Lamia, S.M. Suaad, Effect of thickness on structural and optical properties of Zn<sub>x</sub>Cd<sub>1-x</sub>S thin films prepared by chemical spray pyrolysis, *Int. J. Thin Films Sci. Technol.* 2 (2) (2013) 127–132.
- [20] F. Yakuphanoglu, M. Sekerci, A. Balaban, The effect of film thickness on the optical absorption edge and optical constants of the Cr(III) organic thin films, *Opt. Mater. (Amst)* 27 (8) (2005) 1369–1372.
- [21] A. Jafari, A. Zakaria, Z. Rizwan, M. Sabri, M. Ghazali, Effect of low concentration Sn doping on optical properties of CdS films grown by CBD technique, *Int. J. Mol. Sci.* 12 (9) (2011) 6320–6328.
- [22] A.O. Flores, P. Bartolo, R. Castro, A.I. Oliva, Annealing effects on the mass diffusion of the CdS/ITO interface deposited by chemical bath deposition, *Rev. Mex. Física* 52 (1) (2006) 15–19.
- [23] S.R. Ferrá-González, D. Berman-Mendoza, R. García-Gutiérrez, S.J. Castillo, R. Ramírez-Bon, B.E. Gnade, M.A. Quevedo-López, Optical and structural properties of CdS thin films grown by chemical bath deposition doped with Ag by ion exchange, *Optik (Stuttg)* 125 (4) (2014) 1533–1536.
- [24] F. Ouachtari, A. Rmili, B. Elidrissi, A. Bouaoud, H. Erguip, P. Elies, Influence of bath temperature, deposition time and S/Od ratio on the structure, surface morphology, chemical composition and optical properties of CdS thin films elaborated by chemical bath deposition, *J. Mod. Phys.* 2 (9) (2011) 1071–1082.
- [25] H. Metin, H. Metin, A. Mehmet, S. Erat, S. Durmus, M. Bozoklu, A. Braun, The effect of annealing temperature on the structural, optical, and electrical properties of CdS films, issue 1: photocatalysis for energy and environmental sustainability, *J. Mater. Res.* 25 (2010) 189–196.
- [26] K.E. Nieto-Zepeda, A. Guillén-Cervantes, K. Rodríguez-Rosales, J. Santos-Cruz, D. Santos-Cruz, M. de la L. Olvera, O. Zelaya-Ángel, J. Santoyo-Salazar, L. A. Hernández-Hernández, G. Contreras-Puente, F. de Moure-Flores, Effect of the sulfur and fluorine concentration on physical properties of CdS films grown by chemical bath deposition, *Results Phys.* 7 (2017) 1971–1975.
- [27] P. Raji, K. Ramachandran, The effect of annealing on the thermal properties of nano-CdS by photoacoustics, *Int. J. Nano Sci.* 6 (1) (2007) 51–56.
- [28] C. Vatankhah, A. Ebadi, Quantum size effects on effective mass and band gap of semiconductor quantum dots, *Res. J. Recent Sci.* 2 (1) (2013) 21–24.
- [29] P.E. Lippens, M. Lannoo, Calculation of the band gap for small CdS and ZnS crystallites, *Phys. Rev. B* 39 (15) (1989) 10935–10942.
- [30] R.S. Mane, C.D. Lokhande, Chemical deposition method for metal chalcogenide thin films, *Mater. Chem. Phys.* 65 (1) (2000) 1–31.
- [31] B.R. Srinivasa, B.K. Rajesh, V.R. Rajagopal, T.R. Subba, Preparation and characterization of CdS nanoparticles by chemical co-precipitation technique, *Chalcogenide Lett.* 8 (3) (2011) 177–185.
- [32] J.-F. Han, C. Liao, L.-M. Cha, T. Jiang, H.-M. Xie, K. Zhao, M.-P. Besland, TEM and XPS studies on CdS/CIGS interfaces, *J. Phys. Chem. Solids* 75 (12) (2014) 1279–1283.
- [33] A. Hasnat, J. Podder, Optical and electrical characteristics of pure CdS thin Films for different thicknesses, *J. Bangl. Acad. Sci.* 37 (1) (2013) 33–41.
- [34] J.C. Osuwa, C.I. Oriaku, I.A. Kalu, Variation of optical band gap with post deposition annealing in CdS/PVA thin films, *Chalcogenide Lett.* 6 (9) (2009) 433–436.
- [35] Y.S. Park, D.C. Reynolds, Exciton structure in photoconductivity of CdS, CdSe and CdS:Se single crystals, *Phys. Rev.* 132 (4) (1963) 2450–2457.
- [36] M.A. Mahdi, J.J. Hassan, N.M. Ahemed, S.S. Ng, Z. Hassan, Growth and characterization of CdS single crystalline micro rod photodetector, *Superlatt. Microstruct.* 54 (2013) 137–145.
- [37] L. John, Recombination process in cadmium sulfide, *Phys. Rev.* 98 (4) (1955) 985–992.
- [38] J.S. Jie, W.J. Zhang, Y. Jiang, X.M. Meng, Y.Q. Li, S.T. Lee, Photoconductive characteristics of single-crystal CdS nanoribbons, *Nano Lett.* 6 (9) (2006) 1887–1892.
- [39] Ho S. Bhushan, A. Oudhia, Photoconductivity and photoluminescence in chemically deposited films of CdS:Se:Cl<sub>2</sub>, *Opto–Electron. Rev.* 17 (1) (2009) 30–39.
- [40] M. Azhar, G.A. Nowsherwan, M.A. Iqbal, S. Ikram, A.F. Butt, M. Khan, N. Ahmad, S.O. Hussain, M.A. Raza, J.R. Choi, S. Riaz, S. Naseem, Morphological, photoluminescence, and electrical measurements of rare-earth metal-doped cadmium sulfide thin films, *ACS Omega* 8 (39) (2023) 36321–36332.
- [41] H. Zhang, X. Mi, B. Kang, Y. Wu, T. Zhang, P. Liu, X. Sun, Z.I. Zhang, N. Liu, H. Xu, Surface-ligand-modified CdSe/CdS nanorods for high-performance light-emitting diodes, *ACS Omega* 8 (4) (2023) 3762–3767.
- [42] K. Hani, O. Isaiah, C. Guangyu, L. Lee, Characterization of CdS thin film grown by CBD using four different cadmium sources, *Thin Solid Film* 516 (2008) 7306–7312.
- [43] A.L. Fahrenbruch, R.H. Bube, *Fundamentals of Solar Cells*, 1st edn, Academic Press, New York, 1983.
- [44] A.S. Nazar, N. Ali, K. Ambrina, A.S. Waqar, Comparative study of CdS thin film at room temperatures fabricated by CSS technique, *World Appl. Sci. J.* 28 (4) (2013) 548–553.
- [45] S.V. Gopi, N. Spalatu, M. Basnayaka, R. Krautmann, A. Katerski, R. Josepson, R. Grzibovskis, A. Vembris, M. Krunks, I. Oja Acik, Post deposition annealing effect on properties of CdS films and its impact on CdS/Sb<sub>2</sub>Se<sub>3</sub> solar cells performance, *Front. Energy Res.* 11 (2023) 1162576.
- [46] M. Ichimura, F. Goto, E. Arai, Structural and optical characterization of CdS films grown by photochemical deposition, *J. Appl. Phys.* 85 (1999) 7411–7417.
- [47] H. Metin, S. Erat, S. Durmus, M. Ari, Annealing effect on CdS/SnO<sub>2</sub> films grown by chemical bath deposition, *Appl. Surf. Sci.* 256 (2010) 5076–5081.
- [48] S. Elmas, S. Ozcan, S. Ozder, V. Bilgin, Influence of annealing temperature on the electrical and optical properties of CdS thin films, *Acta Phys. Polon. A* 121 (2012) 56–58.
- [49] I. Yu, T. Isobe, M. Seena, Preparation and properties of CdS thin films comprising nano-particles by a solution growth technique, *Mater. Res. Bull.* 30 (8) (1995) 975–980.
- [50] U.D. Quinonez, A. Vera-Marquina, D. Berman-Mendoza, L.A. Leal-Cruz, L. A. Garcia-Delgado, I.E. Zaldivar-Huerta, A. Garcia-Juarez, A.G. Rojas-Hernandez, R. Gomez-Fuentes, Annealing effect on structural, morphological, and optical behaviors of CBD-CdS nanostructured films for solar cells, *Opt. Mater. Express* 4 (11) (2014) 2280–2289.
- [51] A. Tanushevski, H. Osmani, CdS thin films obtained by chemical bath deposition in the presence of fluorine and the effect of annealing on their properties, *Chalcogenide Lett.* 15 (2) (2018) 107–113.
- [52] K. Balashangar, M. Thanihachelvan, P. Ravirajan, G.D.K. Mahanasa, M.A.K. L. Dissanayake, E. Colegrove, R.G. Dhere, S. Sivananthan, The effect of surface roughness of substrates on the performance of polycrystalline cadmiumsulfide/cadmium telluride solar cells, *J. Nanoelectron. Optoelectron.* 10 (2015) 1–5.
- [53] Z. Fang, X.C. Wang, H.C. Wu, C.Z. Zhao, Achievements and challenges of CdS/CdTe solar cells, *Thin-Film Photovolt.* (2011) 297350.
- [54] K. Rodríguez-Rosales, J.G. Quinones-Galván, A. Guillén-Cervantes, E. Campos-González, J. Santos-Cruz, S.A. Mayén-Hernández, J.S. Arias-Cerón, M.L. Olvera, O. Zelaya-Angel, L.A. Hernández-Hernández, G. Contreras-Puente, F. de Moure-Flores, Nanocrystalline-CdS thin films grown on flexible PET-substrates by chemical bath deposition, *Mater. Res. Express* 4 (2017) 075904.
- [55] K.E. Nieto-Zepeda, J.G. Quinones-Galván, K. Rodríguez-Rosales, A. Guillén-Cervantes, J. Santos-Cruz, O. Zelaya-Ángel, F. de Moure-Flores, Optoelectronic properties of Cl and F doped CdS thin films grown by chemical bath deposition, *Optik (Stuttg)* 226 (2021) 166004.
- [56] L.A. Carrasco-Chavez, J.F. Rubio-Valle, A. Jiménez-Pérez, J.E. Martín-Alfonso, A. Carrillo-Castillo, Study of CdS/CdS nanoparticles thin films deposited by soft chemistry for optoelectronic applications, *Micromachines (Basel)* 14 (2023) 1168.
- [57] J.-F. Han, C. Liao, L.-M. Cha, T. Jiang, H.-M. Xie, K. Zhao, M.-P. Besland, TEM and XPS studies on CdS/CIGS interfaces, *J. Phys. Chem. Solids* 75 (12) (2014) 1279–1283.

- [58] A.A. Al-mebir, P.H. Ali Kadhim, G. Zeng, J. Wu, Effect of *In Situ* thermal annealing on structural, optical, and electrical properties of CdS/CdTe thin film solar cells fabricated by pulsed laser deposition, *Adv. Condens. Matter Phys.* 2016 (2016) 8068396.
- [59] R. Prasanna-Kumari, D. Herrera-Molina, A. Fernández-Pérez, J.E. Diosa, E. Mosquera-Vargas, Study of the properties of CdS:Al (R = [Al<sup>3+</sup>]/[Cd<sup>2+</sup>] = 0.30, 0.40, 0.50), thin films grown by the CBD method in an ammonia-free system, *Molecules* 28 (8) (2023) 3626.
- [60] H. Li, X. Liu, Improved performance of CdTe solar cells with CdS treatment, *Sol. Energy* 115 (2015) 603–612.